RESEARCH PAPER

In vitro Phase I and Phase II metabolism of α-pyrrolidinovalerophenone (α-PVP), methylenedioxypyrovalerone (MDPV) and methedrone by human liver microsomes and human liver cytosol

Noelia Negreira[1] · Claudio Erratico[1] · Tina Kosjek[2] · Alexander L. N. van Nuijs[1] ·
Ester Heath[2] · Hugo Neels[1] · Adrian Covaci[1]

Abstract The aim of the present study was to identify the in vitro Phase I and Phase II metabolites of three new psychoactive substances: α-pyrrolidinovalerophenone (α-PVP), methylenedioxypyrovalerone (MDPV), and methedrone, using human liver microsomes and human liver cytosol. Accurate-mass spectra of metabolites were obtained using liquid chromatography-quadrupole time-of-flight mass spectrometry. Six Phase I metabolites of α-PVP were identified, which were formed involving reduction, hydroxylation, and pyrrolidine ring opening reactions. The lactam compound was the major metabolite observed for α-PVP. Two glucuronidated metabolites of α-PVP, not reported in previous in vitro studies, were further identified. MDPV was transformed into 10 Phase I metabolites involving reduction, hydroxylation, and loss of the pyrrolidine ring. Also, six glucuronidated and two sulphated metabolites were detected. The major metabolite of MDPV was the catechol metabolite. Methedrone was transformed into five Phase I metabolites, involving N- and O-demethylation, hydroxylation, and reduction of the ketone group. Three metabolites of methedrone are reported for the first time. In addition, the contribution of individual human CYP enzymes in the formation of the detected metabolites was investigated.

Introduction

An increasing number of new psychoactive substances (NPS) have been recently introduced into the drug market [1]. These NPS are mostly synthetic and mimic the effects of conventional illicit drugs (e.g., cannabis, amphetamines, cocaine, etc.), sometimes by simply adding or changing a functional group of already known psychoactive substances [1, 2]. Among them, the presence of synthetic cathinones on the European drug market was noted for the first time in 2009 [3]. Synthetic cathinones are a group of derivatives of cathinone, a phenylalkylamine alkaloid naturally present in *Catha edulis* [4–6]. Cathinone causes amphetamine-like sympathomimetic effects, including tachycardia and hypertension as well as psychoactive effects such as euphoria and increased alertness [1].

One of the most known synthetic cathinones is methylenedioxy-pyrovalerone (MDPV), a potent monoamine transporter blocker with stimulating effects [7, 8]. Several MDPV analogues have appeared on the market, including the popular and widespread α-pyrrolidinovalerophenone (α-PVP) [9]. Besides MDPV, mephedrone (4-methyl-methcathinone) was also one of the first introduced and most used NPS [10], but recently, its demand decreased because of legislative actions and an analogue, known as methedrone (4-methoxy methylcathinone), has entered the market [11, 12]. In

✉ Adrian Covaci
adrian.covaci@uantwerpen.be

[1] Toxicological Center, Department of Pharmaceutical Sciences, University of Antwerp, Universiteitsplein 1, 2610 Wilrijk, Antwerp, Belgium

[2] Department of Environmental Sciences, Jozêf Stefan Institute, Jamova 39, 1000 Ljubljana, Slovenia

spite of their recent introduction, deaths associated with the use of these NPS were already reported [13–18].

NPS may undergo extensive metabolism in the body, leading to low or even negligible levels of the parent compound in urine [19]. For this, the detection and quantification of metabolites constitutes, in many cases, the only possible way to get useful information on the use of these substances. To this end, the use of in vitro metabolism experimental setups, using human liver microsomes (HLM) and high-performance liquid chromatography (HPLC) coupled to accurate-mass mass spectrometry (AMMS) has proven to be a useful approach for the characterization of the metabolism of MDPV [20, 21] and α-PVP [22]. However, AMMS was not used in the case of methedrone.

Although some information on the in vitro metabolism of MDPV, α-PVP, and methedrone is available, several important research gaps are still present. First, out of the 12 Phase I metabolites MDPV detected in a urine sample from an MDPV user [21], only two were identified in vitro human metabolism [20]. Second, out of the seven Phase I metabolites detected in urine samples from α-PVP users [23], five were confirmed in in vitro experiments [22]. Third, CYP-mediated in vitro metabolism of methedrone was investigated [24] and two metabolites were identified, one of which was also found in urine samples from two fatal intoxications [13]. However, the confirmation of these metabolites was not done by AMMS. In addition, no Phase II metabolism was investigated in vitro or in vivo for α-PVP and methedrone. Cytochrome-P450 (CYP) enzymes involved in the formation of Phase I metabolites was investigated only for major MDPV metabolites identified [21]. Full characterization of the in vitro metabolism pathway of drugs is of key importance because their Phase I and Phase II metabolites are the most likely urinary biomarkers of human drug consumption. The identification of the (CYP) enzymes involved in drug metabolism is also of great importance to describe (and predict) drug-to-drug interaction and sublethal effects.

To address these issues, the aim of this study was to investigate the in vitro Phase I and Phase II metabolism of MDPV, α-PVP and methedrone by HLM and human liver cytosol (HLCYT). Metabolites were identified through liquid chromatography coupled to accurate mass spectrometry measurements using QTOF. In addition, the involvement of individual human CYP enzymes in the formation of Phase I metabolites was studied using a panel of human recombinant CYPs (rCYPs).

Material and methods

Chemicals and reagents

Chemical standards of α-PVP and methedrone were obtained from Cerilliant (Round Rock, TX, USA) at a concentration of 1 mg/mL in methanol, whereas MDPV was purchased from TRC (Toronto, Canada) in neat powder. The internal standard, theophylline, was obtained as powder (anhydrous, >99 % pure) from Sigma-Aldrich (Diegem, Belgium). Pooled HLM (mix gender, n=200) was purchased from Tebu-bio (Boechout, Belgium). Pooled HLCYT (mix gender, n=200), chemical standards for 2,6-uridinediphosphate glucuronic acid (UDPGA), alamethicin (neat, purity>99 %), adenosine 3′-phosphate 5′-phosphosulphate (PAPS; neat, purity>60 %) lithium salt hydrate, 4-nitrophenol (4-NP), 4-nitrophenol-glucuronide (4-NP-Gluc; neat, purity>99 %), 4-nitrophenol-sulphate (4-NP-Sulf; neat, purity>99 %), and NADPH (neat, purity>99 %) were purchased from Sigma-Aldrich (Diegem, Belgium). Baculovirus-insect cell microsomes containing expressed human CYP enzyme (CYP1A2, 2B6, 2C9, 2C19, 2D6, 2E1, or 3A4) coexpressed with human CYP oxidoreductase and human cytochrome b5 were purchased from BD Biosciences (Erembodegem, Belgium) and Tebu-Bio. Ultrapure water was obtained using a Purelab flex water system by Elga (Tienen, Belgium). Acetonitrile and formic acid were purchased from Merck (Darmstadt, Germany). All organic solvents were HPLC grade or higher.

In vitro metabolism assays

The formation of Phase I metabolites by CYP enzymes was studied. The reaction mixture (final volume: 1 mL), consisting of 100 mM TRIS-HCl buffer (pH adjusted to 7.4 at 37 °C), HLM (final concentration: 0.5 mg/mL) and the individual drug (final concentration: 10 μM) was prepared on ice and then pre-incubated for 5 min in a shaking water bath at 37 °C. The reaction was initiated by addition of 10 μL of NADPH solution (final concentration: 1 mM) in the mixture. To stop the reaction after 3 h, 250 μL of an ice-cold acetonitrile solution containing 1 % formic acid and 5.0 μg/mL of theophylline (used as internal standard) was added to each sample, which was then vortex-mixed for 30 s and centrifuged at 8000 rpm for 5 min. The supernatant was then transferred to a glass tube, concentrated to dryness under a gentle stream of nitrogen gas at 60 °C, and reconstituted with 200 μL ultrapure water before transferring it to an HPLC vial for analysis.

The formation of Phase II metabolites was investigated in two steps. First, Phase I metabolites were produced by incubating substances with HLMs and NADPH as described above. This reaction was quenched by putting the samples on ice for 5 min. Samples were then centrifuged at 8000 rpm for 5 min and 940 μL of the supernatant containing the fraction of non-metabolized drug and its formed Phase I metabolites was transferred to a tube containing fresh pooled HLM or pooled HLCYT (final concentration: 0.5 mg/mL) to investigate uridinediphosphate glucuronic acid transferase (UGT) or sulfotransferase (SULT) mediated metabolism, respectively. The reaction mixture was prepared as described

above for CYP enzyme samples, but adding (only in the samples focusing on UGT enzymes) a 10 μL aliquot of alamethicin (final concentration: 10 μg/mL) dissolved in dimethyl sulphoxide (1 % DMSO, final concentration) before pre-incubating the samples in the water bath. Also, the reaction was started by addition of UDPGA or PAPS co-factors (1 mM, final concentration) to activate UGTs and SULTs, respectively. Samples were incubated for 3 h and further prepared as described above.

Further experiments were carried out by incubating the substances with HLM over a range of incubation times (10, 20, 40, 60, and 90 min), enzyme concentrations (0.2, 0.4, 0.6, and 0.8 mg/mL) and substrate concentrations (1, 3, 5, and 10 μM) to monitor the consistent formation of Phase I metabolites over a range of different incubation conditions.

Positive and negative control samples for each enzyme family were prepared under the same conditions as earlier described in order to assure adequate experimental procedures. In the positive control samples for UGT and SULT activity, 4-nitrophenol was selected as substrate and formation of 4-nitrophenol-glucuronide [25] and 4-nitrophenol-sulphate [26], respectively, was monitored. Positive control samples were not prepared for CYP enzymes because the activity of the major ten CYPs present in HLM was previously characterized by the manufacturer (data not shown). Negative control samples were prepared for each family of enzymes by replacing enzymes, substrate, or the cofactor with an equivalent aliquot of buffer or acetonitrile in order to avoid false-positive results.

The role of individual human CYP enzymes was investigated using a panel of human rCYPs, including human rCYP1A2, 2B6, 2C9, 2C19, 2D6, 2E1, and 3A4. Reaction mixtures were prepared as described above, but using one human rCYP (20 pmol/mL, final concentration) instead of HLMs. The reaction was allowed to proceed for 1 h. Negative control samples were prepared replacing the human rCYP with an equivalent aliquot of buffer.

Liquid chromatography accurate-mass spectrometry

Identification of potential metabolites was performed using LC coupled to a QTOF-MS with electrospray ionisation (ESI). The apparatus consisted of a 1290 Infinity LC (Agilent Technologies, Wilmington, DE, USA) connected to a 6530 Accurate-Mass QTOF-MS (Agilent Technologies) with a heated-ESI source (JetStream ESI).

Chromatographic separation was performed on a C_8 Zorbax Eclipse Plus column (150×2.1 mm, 3.5 μm) from Agilent Technologies, maintained at 30 °C, and using a mobile phase composed of 0.1 % of formic acid in ultrapure water (A) and acetonitrile (B) with the following gradient: 0–5 min: 3 % B; 5–30 min: 3 %–50 % B; 30–31 min: 50 %–100 % B; 31–33 min: 100 % B; 33–34 min: 100 %–3 % B; 34–40 min:

3 % B. The flow rate and the injection volume were set at 0.18 mL/min and 5 μL, respectively.

The QTOF-MS instrument was operated in the 2 GHz (extended dynamic range) mode, which provides a full width at half maximum (FWHM) resolution of approximately 4700 at m/z 118 and 10,000 at m/z 922. Both polarity ESI modes were used under the following specific conditions: gas temperature 300 °C; gas flow 8 L/min; nebulizer pressure 40 psi; sheath gas temperature 325 °C; sheath gas flow 11 L/min. Capillary and fragmentor voltages were set to 3500 and 100 V, respectively. A reference calibration solution (provided by Agilent Technologies) was continuously sprayed into the ESI source of the QTOF-MS system. The ions selected for recalibrating the mass axis, ensuring the mass accuracy throughout the run were m/z 121.0508 and 922.0097 for positive mode and m/z 112.9856 and 966.0007 for negative mode. The QTOF-MS device was acquiring from m/z 50 to 1000 in MS mode and from m/z 40 to 500 in data-dependent acquisition mode (auto-MS/MS) using three different collision energies (10, 20, and 40 eV) for the fragmentation of the selected parent ions. The maximum number of precursors per MS cycle was set to three with minimal abundance of 2000 counts. In addition, precursor ions were excluded after every three spectra and released after 0.6 min. An exclusion list with ions present in the substrate negative control was also used. For some metabolites, additional injections in targeted MS/MS were necessary in order to obtain proper MS/MS fragmentation data.

Post-acquisition data processing

Metabolite identification was based on mass accuracy and isotopic abundance obtained in MS mode, on the MS/MS fragmentation patterns and the accurate masses of the product ions, and on the predicted $logK_{ow}$ by ChemBio3D Ultra. The MassHunter Workstation software (Agilent Technologies) and XCMS online (open-source software from Scripps Center for Metabolomics) were used to process the obtained data and to provide an automated detection of metabolites, respectively. The XCMS software aligns the total ion current chromatograms (TICCs) corresponding to the negative controls and to the samples, and determines if there is a statistically significant difference between control and sample. A complete workflow can be found elsewhere [27]. A list of putative metabolites is proposed and the change in response between the control and real samples can be visualized on extracted ion chromatograms. Following this automated analysis, the raw data were examined by manual processing in MassHunter, using a mass window of 10 ppm around the precursor ion. Nexus v1.5 (Lhasa Ltd.) software was also considered in order to have a first prediction of plausible metabolites.

Results and discussion

Detection and identification of metabolites

TICCs of the samples were compared with negative controls. Visual inspection of these chromatograms showed no clear differences between them. Thus, in order to facilitate this search and speed it up, the data analysis, a workflow based on the XCMS software was applied. The identified metabolites of α-PVP, MDPV, and methedrone are listed in Tables 1, 2, and 3, respectively. Sulphated metabolites were analyzed in negative mode, whereas all other metabolites were analyzed in positive mode. The chemical structure of the detected metabolites was postulated by interpretation of the mass shifts in the MS/MS spectra in relation to the MS/MS spectrum of the parent compound and in accordance with previously published data [21–23, 28–30]. Figures S1 to S3 in the Electronic Supplementary Material (ESM) show the MS/MS spectra of the three substances and their detected metabolites. Extracted ion chromatograms (EICs) of the identified metabolites are showed in ESM Figs. S4 to S6.
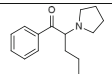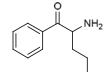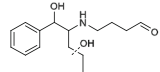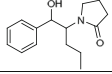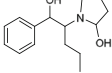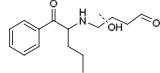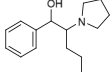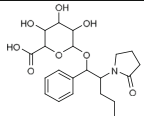
α-PVP

The fragmentation pattern of α-PVP was in agreement with previously published data [31] with major fragments observed at m/z 126.1271 (Δm=−4.76 ppm), 105.0333 (Δm=−1.90 ppm), 91.0540 (Δm=−2.20 ppm), and 77.0385

(Δm=−1.30 ppm) (ESM Fig. S1). The in vitro CYP-catalyzed metabolism for α-PVP yielded six potential metabolites (Table 1 and ESM Fig. S1). Metabolite M1 was formed through a transformation of the pyrrolidine ring into a primary amine, resulting in m/z 178.1226 (Δm=3.31 ppm). This metabolite was also detected in the in vitro study performed by Tyrkkö et al. [22] and in rat urine by Sauer et al. [29], but not in human urine [22, 23]. Uralets et al. [31] did not find M1 in human urine, but they found a metabolite formed after reduction of the ketone group leading to an alcohol. The fragmentation pattern of M1 and α-PVP have similarities as evidenced from the presence of m/z 105.0350 (Δm=14.28 ppm) and 91.0560 (Δm=19.77 ppm). However, the most abundant fragments at m/z 160.1134 (Δm=8.12 ppm) and 130.0831 (Δm=5.38 ppm) are specific for M1 (Table 1 and ESM Fig. S1).

M2 was formed through a combination of reactions: a reduction/hydrogenation of α-PVP, a hydroxylation of the pyrrolidine ring, followed by an oxidation and ring opening with an additional hydroxylation. The fragments at m/z 248.1649 (Δm=1.61 ppm) and 230.1551 (Δm=5.21 ppm) showed two successive and very favorable losses of water, which means that the structure contained two secondary hydroxyl groups. An additional loss of a CO moiety at m/z 202.1628 (Δm=18.80 ppm) indicated the existence of an aldehyde group. The fragment at m/z 188.1066 (Δm=−2.13 ppm) is due to the loss of the propyl side chain from m/z 230.1551, indicating that the aldehyde group was located

Table 1 Postulated structures for α-PVP and its Phase I and Phase II metabolites

Compound	Retention time (min)	Theoretical m/z [M+H]+	Measured m/z [M+H]+	Error (ppm)	Diagnostic product ions	Chemical formula	Structure	Log Kow[1]
α-PVP	18.79	232.1696	232.1703	3.06	126.1271, 105.0333, 91.0540, 77.0385	$C_{15}H_{21}NO$		3.31
M1	15.78	178.1226	178.1232	3.31	160.1134, 130.0831	$C_{11}H_{15}NO$		2.19
M2	16.12	266.1751	266.1756	2.10	248.1649, 230.1551, 202.1628, 188.1066	$C_{15}H_{23}NO_3$		1.68
M3	16.63	248.1645	248.1650	2.10	230.1532, 202.1569, 118.0657, 142.1197	$C_{15}H_{21}NO_2$		2.21
M4	17.09	250.1802	250.1807	2.28	232.1721, 214.1608, 172.1132, 160.1142, 130.0672	$C_{15}H_{23}NO_2$		2.49
M5	17.54	264.1594	264.1599	1.93	246.1471, 186.0910	$C_{15}H_{21}NO_3$		2.38
M6	18.75	234.1852	234.1858	2.52	216.1726, 173.1176, 72.0801	$C_{15}H_{23}NO$		3.02
M3-GLU	14.66, 15.20	424.1966	424.1966 / 424.1996	4.46 / 7.07	248.1593, 230.1501, 105.0347, 91.0548 / 248.1601, 230.1490, 105.0316, 91.0541	$C_{21}H_{29}NO_8$		0.94

[a] Estimated by ChemBio3D Ultra.

Table 2 Postulated structures for MDPV and its Phase I and Phase II metabolites

Compound	Retention time (min)	Theoretical m/z [M+H]+	Measured m/z [M+H]+	Error (ppm)	Diagnostic product ions	Chemical formula	Structure	logKow[1]
MDPV	19.17	276.1594	276.1594	0.00	205.0866, 175.0762, 149.0242, 135.0448, 126.1289, 84.0821	$C_{16}H_{21}NO_3$		3.06
M1	12.56	280.1543	280.1544	0.36	262.1458, 191.0703, 139.0390, 109.0283, 72.0813	$C_{15}H_{21}NO_4$		1.70
M2	13.21	264.1599	264.1605	2.27	175.0762, 137.0246, 126.1291, 123.0454, 109.0302	$C_{15}H_{21}NO_3$		2.92
M3	14.20	262.1438	262.1439	0.38	220.0987, 178.0514, 145.0662, 127.0547	$C_{15}H_{19}NO_3$		2.49
M4	16.15	310.1649	310.1636	-4.19	292.1556, 274.1461, 246.1493, 175.0736, 149.0243, 71.0498	$C_{16}H_{23}NO_5$		1.14
M5	16.25	222.1125	222.1112	-5.85	204.1002, 174.0900, 146.0941, 117.0552, 135.0426	$C_{12}H_{15}NO_3$		1.94
M6	16.79	260.1281	260.1272	-3.46	230.0812, 202.0851, 156.0799	$C_{15}H_{17}NO_3$		3.00
M7	17.14	292.1543	292.1547	1.37	274.1467, 205.0853, 149.0243, 142.1233, 135.0454, 121.0299, 70.0670	$C_{16}H_{21}NO_4$		2.53, 2.05
M8	17.49	294.1700	294.1697	-1.02	276.1583, 258.1461, 246.1491, 204.1012, 174.0815, 149.0236, 135.0439	$C_{16}H_{23}NO_4$		1.55
M9	17.86	308.1498	308.1495	-0.97	290.1397, 272.1275, 260.1279, 214.1227, 187.0758, 149.0234, 135.0441, 140.1073	$C_{16}H_{21}NO_5$		1.31
M10	18.61	278.1751	278.1733	-6.47	260.1678, 217.1126	$C_{16}H_{23}NO_3$		2.76
M2-GLUa	9.55	440.1915	440.1921	1.36	264.1611, 193.0878, 126.1307, 72.0835	$C_{21}H_{29}NO_9$		0.95
M2-GLUb	11.21		440.1938	5.22	264.1588, 193.0863, 126.1288, 72.0829			
M2-SULa[2]	13.42	342.1017	342.1003	-4.09	262.1460, 193.0826, 163.0409, 136.0158, 108.0214	$C_{15}H_{21}NO_6S$		1.40
M2-SULb[2]	14.21		342.1017	0.00	262.1457, 193.0397, 136.0155, 108.0219			
M3-GLUa	8.73	438.1759	438.1766	1.60	262.1440, 234.1491	$C_{21}H_{27}NO_9$		0.53
M3-GLUb	9.41		438.1758	-0.23	262.1459, 234.1518			
M6-GLUa	13.46	436.1602	436.1590	-2.75	260.1307	$C_{21}H_{25}NO_9$		1.04
M6-GLUb	14.35		436.1616	3.21	260.1284			

[a] Estimated by ChemBio3D Ultra.

[b] Data in negative mode.

in the longer chain. At the same time, only a double bond was present, suggesting that the other hydroxylation took place in the propyl side chain. To the best of our knowledge, M2 is reported for the first time in the present study.

M3 *(m/z 248.1650, Δm=2.10 ppm)* corresponded to the reduction of α-PVP combined with a hydroxylation in the pyrrolidine ring and a subsequent oxidation. A minor peak of M3 detected just before M3 and with an identical MS/MS

Table 3 Postulated structures for methedrone and its Phase I metabolites

Compound	Retention time (min)	Theoretical m/z $[M+H]^+$	Measured m/z $[M+H]^+$	Error (ppm)	Diagnostic product ions	Chemical formula	Structure	logKow[1]
Methedrone	18.71	194.1181	194.1190	4.64	176.1072, 161.0835, 146.0602, 132.0809, 118.0654, 103.0530, 91.0552, 77.0397	$C_{11}H_{15}NO_2$	(structure)	1.58
M1	7.27	182.0812	182.0816	2.20	165.0560, 147.0439, 136.0772, 123.0447, 107.0509, 91.0553, 77.0396	$C_9H_{11}NO_3$	(structure)	-0.24
M2	8.94	210.1130	210.1121	-4.28	-	$C_{11}H_{15}NO_3$	(structure)	0.45
M3	12.95	180.1024	180.1018	-3.33	162.0905, 147.0682, 132.0466, 121.0639, 117.0575, 103.0561, 91.0550, 77.0390	$C_{10}H_{13}NO_2$	(structure)	1.20
M4	17.48	180.1024	180.1023	-0.56	162.0906, 147.0673, 132.0431, 118.0656, 104.0491, 91.0543, 77.0391	$C_{10}H_{13}NO_2$	(structure)	1.27
M5	18.27	196.1337	196.1341	2.04	178.1226, 146.0964	$C_{11}H_{17}NO_2$	(structure)	1.29

[a] Estimated by ChemBio3D Ultra. − no data.

spectrum indicated isomerism as previously reported in HLM experiments [22] and in human [23] and rat urine [29].

M4 (m/z 250.1807, Δm=2.28 ppm) was formed from α-PVP through a reduction and a hydroxylation. This metabolite was also reported in the study by Tyrkkö et al. [22], but information about its fragmentation pattern was lacking. The fragments at m/z 232.1721 (Δm=10.77 ppm) and 214.1608 (Δm=8.40 ppm) indicated the loss of one and two water molecules, respectively. Subsequently, the loss of the propyl side chain (m/z 172.1132, Δm=6.39 ppm), the pyrrolidine ring (m/z 160.1142, Δm=13.12 ppm), or both (m/z 130.0672, Δm=16.15 ppm and m/z 118.0665, Δm=11.86 ppm) were observed. The ions at m/z 105.0355 (Δm=19.04 ppm), 91.0561 (Δm=20.87 ppm), and 77.0409 (Δm=29.86 ppm) were similar to the α-PVP MS/MS spectrum. In some cases, the mass errors were higher than 20 ppm, probably due to the low abundance observed for this metabolite. M4 was not identified in human [22] and rat urine [29] samples, suggesting a minor role of this metabolite in vivo.

The formation of M5 (m/z 264.1599, Δm=1.93 ppm) from α-PVP can be explained from a combination of reactions: a hydroxylation of the pyrrolidine ring, an oxidation, a ring opening, and an additional hydroxylation. Tyrkkö et al. [22] observed the same exact mass in their in vitro experiments, but the structure was assigned to the formation of a carboxylic acid due to a loss of water, acetic acid, and amino-butyric acid. In our case, only the loss of water was faintly observed at m/z 246.1471 (Δm=−7.31 ppm) but the other losses, including a possible loss of CO_2, were not seen. The fragment at m/z 186.0910 (Δm=−1.61 ppm) indicated that the hydroxyl and carbonyl groups were in the aminobutyl side chain because of the presence of two double bonds. However, the exact position of the hydroxyl group could not be elucidated.

M6 (m/z 234.1858, Δm=2.52 ppm) was formed through a reduction of the ketone moiety of α-PVP. A loss of water and a subsequent loss of the propyl side chain as a cation radical led to ions at m/z 216.1726 (Δm=−9.71 ppm) and 173.1176 (Δm=−13.29 ppm), respectively, as previously reported by Tyrkkö et al. [22]. The presence of the ion at m/z 72.0801 (Δm=−9.71 ppm) supports the hypothesis that the pyrrolidine ring remained unaltered here. This metabolite was the most abundant metabolite found in in vitro [22] and in vivo [22, 23] studies.

An additional metabolite (m/z 246.1489), formed by a hydroxylation followed by a dehydrogenation, was reported in in vitro experiments [22] and was also observed in human urine [23]. This metabolite was, however, not observed in the present study, but it could be formed as an intermediate between the parent compound and M5. In addition, the oxidation of the two hydroxyl groups led to m/z 250.18073 observed in our study (M4). Drug and protein concentrations used in the in vitro experiments by Tyrkkö et al. [22] (100 μM and 2 mg/mL, respectively) were higher than those used in the present study (10 μM and 0.5 mg/mL) and our incubation time was shorter. Therefore, differences in experimental setups used in different in vitro metabolism studies could explain the observed differences.

In addition, two putative glucuronide conjugations of M3 were detected in the Phase II experiments. Both metabolites eluted earlier than M3 with m/z 424.1996 (Δm=7.07 ppm)

and 424.2008 (Δm=9.90 ppm). The presence of both metabolites could be a result of isomerism of M3, but they also can originate from two different bonds with the glucuronic acid by a mechanism known as acyl migration [32]. However, no evidence could be found in the MS/MS spectra to support this hypothesis. The fragmentation pattern of the glucuronidated M3 was characterized through the neutral loss of m/z 176 (a glucuronyl group) resulting in M3 at m/z 248.1593 (Δm= −20.95 ppm) and 248.1602 (Δm=−17.33 ppm) for isomer one and two, respectively. In addition, the characteristic fragments of M3 (m/z 230, 105, and 91) were also observed for these glucuronidated conjugates. The mass errors were higher than for Phase I metabolites because the intensity of these conjugated compounds was very low. To the best of our knowledge, the glucuronidated conjugate of M3 was not detected before in in vitro or in vivo studies. On the other hand, the glucuronidated conjugate of M6 was found in human urine [23], but not in the present study.

Sulphated conjugates of α-PVP were not detected in the Phase II experiments. However, the metabolite of 4-NP produced by SULTs (4-NP-SULF) was detected in the positive control sample, demonstrating a good experimental setup and suggesting that sulphation did not occur.

MDPV

The fragmentation pattern for MDPV (ESM Fig. S2) was in agreement with previously published data [12, 20, 21, 28]. The following paragraphs describe the identified metabolites in detail (Table 2 and ESM Fig. S2).

M1 (m/z 280.1544, Δm=0.36 ppm) resulted from MDPV through a loss of the methylene group and subsequent hydroxylation. A loss of water at m/z 262.1458 (Δm=7.63 ppm), followed by subsequent losses, including a loss of methanol at m/z 109.0283 (Δm=−0.92 ppm) and the pyrrolidine ring unaltered at m/z 72.0813 (Δm=6.94 ppm) evidenced that the hydroxylation took place in the alkyl side chain. The loss of the methylene group was indicated by the lack of fragments at m/z 149 and 135, present in the MS/MS spectrum of MDPV. This metabolite was observed in human urine [21, 33] but not in studies investigating the in vitro human metabolism of MDPV [21].

M2 (m/z 264.1605, Δm=2.27 ppm) corresponded to the loss of the methylene group of MDPV. M2 was the major metabolite of MDPV, which was consistent with previous in vitro [20] and in vivo [21, 33] studies. The most abundant ions at m/z 175.0762 (Δm=4.57 ppm), 137.0246 (Δm= 9.49 ppm), 126.1291 (Δm=11.10 ppm), 123.0454 (Δm= 10.57 ppm), and 109.0302 (Δm=16.51 ppm) were already elucidated by Meyer et al. [21].

M3 (m/z 262.1434, Δm=0.38 ppm) was formed from the parent compound by a loss of the methylene group followed by a dehydrogenation in the alkyl chain. Alternatively, it could

also be the result from a dehydration of M1. The lack of ions at m/z 149 and 135 supported the loss of the methylene moiety in the precursor ion. Several ions indicated the formation of a double bond. For instance, the ion at m/z 220.0987 (Δm= 8.63 ppm) corresponded to the loss of a propylene moiety (C_3H_6) instead of a propyl group (C_3H_8). The ion at m/z 178.0514 (Δm=8.42 ppm) may indicate the loss of the pyrrolidine ring and an ethylene moiety. The fragmentation resulting in an ion at m/z 145.0662 (Δm=9.65 ppm) can be explained by the losses of two hydroxyl groups, the pyrrolidine ring and a methane moiety. A subsequent loss of water yielded the ion at m/z 127.0547 (Δm=3.94 ppm), which can be explained by the formation of a naphthalene ring. Successive fragmentations in the naphthalene ring led to different ions also observed in the metabolites as explained above. To the best of our knowledge, the formation of M3 is reported for the first time.

M4 (m/z 310.1636, Δm=−4.19 ppm) was formed after a reduction of the ketone moiety of MDPV followed by two hydroxylations: one in the propyl chain and one in the α-position to the nitrogen atom. A subsequent oxidation of the latter hydroxyl group caused a ring opening. Two consecutive water losses at m/z 292.1556 (Δm=4.45 ppm) and 274.1461 (Δm=8.39 ppm) and a subsequent loss of CO at m/z 246.1493 (Δm=1.63 ppm) indicated the presence of two hydroxyl groups and an aldehyde group. An additional ion at m/z 71.0498 (Δm=9.85 ppm) demonstrated the existence of an aldehyde group in the N-butyl side chain of the parent ion, which indicates ring opening. The fragment at m/z 149.0243 (Δm=6.71 ppm) showed the presence of the methylenedioxybenzoyl moiety similar to MDPV. To the best of our knowledge, formation of M4 is reported for the first time.

M5 (m/z 222.1120, Δm=−5.85 ppm) resulted from the transformation of the pyrrolidine ring of MDPV to a primary amine. The first ion at m/z 204.1002 (Δm=−8.33 ppm) corresponded to a loss of water and can be explained by the formation of a conjugated indole system between the primary amine and the aromatic ring, similar to that observed for M1 of α-PVP. Subsequent losses of a methyleneoxy and methylenedioxy moiety led to the ions at m/z 174.0900 (Δm=−7.47 ppm) and 146.0941 (Δm=−15.74 ppm), respectively. An additional loss of the propyl radical yielded the ion at m/z 117.0552 (Δm=−17.94 ppm). The ion at m/z 135.0426 (Δm=−11.11 ppm) showed the presence of the unchanged methylenedioxy moiety. To the best of our knowledge, this metabolite was not previously reported in vitro or in vivo metabolism studies of MDPV.

M6 (m/z 260.1272, Δm=−3.46 ppm) corresponded to the loss of the methylene group followed by two dehydrogenations. MS/MS fragmentation suggested a loss of the C_2H_6 moiety (m/z 230.0812, Δm=0.00 ppm) followed by a loss of CO (m/z 202.0851, Δm=−5.94 ppm), respectively. The

ion at *m/z* 202 fragmented further to the ion at *m/z* 156.0799 (Δm=−5.77 ppm) after ring opening and formation of a bond between the nitrogen atom and the phenyl ring, yielding an indole system.

M7 (*m/z* 292.1547, Δm=1.37 ppm) corresponded to a hydroxylation of MDPV. A loss of water was observed at *m/z* 274.1467 (Δm=10.58 ppm). The ion at *m/z* 205.0853 (Δm=−2.93 ppm) suggested a hydroxylation of the pyrrolidine ring due to the lack of a double bond in this fragment. The existence of the ions at *m/z* 149.0243 (Δm=6.71 ppm), 135.0454 (Δm=7.40 ppm), and 121.0299 (Δm=4.13 ppm) showed the presence of the unchanged methylenedioxybenzoyl moiety. This metabolite was detected as a product of microbial biotransformation in wastewater [28], but not in human in vitro and in vivo metabolism experiments. Therefore, M7 is reported for the first time to be an in vitro metabolite of MDPV in humans. Meyer et al. [21] attributed the *m/z* 292.1534 to the demethylenyl-methyl-oxo-metabolite in human urine. The ions at *m/z* 151.0389 and 140.1069 appeared in their spectrum [21] instead of 149 and 142.

M8 (*m/z* 294.1697, Δm=−1.02 ppm) is formed from MDPV through a hydrogenation followed by a hydroxylation. It was indicated by two consecutive losses of water at *m/z* 276.1583 (Δm=−3.98 ppm) and 258.1461 (Δm=−10.85 ppm). Subsequently, the methylene group was lost yielding ion at *m/z* 246.1491 (Δm=0.81 ppm). After that, two possible fragments at *m/z* 204.1012 (Δm=−3.43 ppm) could correspond to the loss of the propyl side chain from 246 or the loss of the pyrrolidine ring from 258 after breaking up the bond between the nitrogen atom and its carbon in α-position. The ions at *m/z* 149.0236 (Δm=2.01 ppm) and 135.0439 (Δm=−1.48 ppm) showed the presence of the unchanged methylenedioxybenzoyl moiety. Mardal and Meyer [28] attributed the same exact mass to another transformation product (hydroxylation in the propyl side chain and ring opening), despite the fact that they obtained the same MS/MS spectrum. This equivocal assignment was due to the fact that only the structures of the fragments at *m/z* 204.1019 and 174.0913 were elucidated and that the two losses of water were ignored [28]. Meyer et al. [21] found another metabolite in human urine with the same exact mass as M8 but with a totally different fragmentation pattern corresponding to the demethylenyl-methyl-hydroxy-alkyl-MDPV. Bertol et al. [33] assigned the same metabolite, also in human urine, following the proposal of Meyer et al. [21], but the MS/MS spectrum was not presented. Therefore, careful evaluation of the MS/MS spectrum and proper interpretation of the product ions is very important to reliably identify the structure of the metabolites.

M9 (*m/z* 308.1495, Δm=−0.97 ppm) corresponded to a dihydroxylation of MDPV. Two losses of water at *m/z* 290.1397 (Δm=3.45 ppm) and 272.1275 (Δm=−2.20 ppm) indicated the presence of two hydroxyl groups. A subsequent loss of a

methylene group or the propyl side chain led to the ions at *m/z* 260.1279 (Δm=−0.77 ppm) and 230.0826 (Δm=6.08 ppm), respectively. The ion at *m/z* 272 was fragmented following two different ways. It lost the methylenedioxy moiety and a methyl group from the propyl side chain yielding ion at *m/z* 214.1227 (Δm=0.47 ppm) or it lost the ring pyrrolidine and the hydroxyl group from the ketone moiety leading to the ion at *m/z* 187.0758 (Δm=2.14 ppm). The ions at *m/z* 149.0234 (Δm=0.67 ppm) and 135.0441 (Δm=0.00 ppm) demonstrated the unchanged methylenedioxy moiety. The presence of the ion at *m/z* 140.1073 (Δm=2.14 ppm), with 2 u of difference compared th the ion at *m/z* 142 shown for M7, indicated the existence of a double bond in the pyrrolidine ring or in the propyl side chain, probably due to the presence of a hydroxyl group. This metabolite was not found previously in in vitro [20] and in vivo [21, 33] experiments. However, evidence of the formation of this compound can be found in the work of Mardal and Meyer [28], where the TOF-MS spectrum was assigned to the hydroxyl-alkyl-oxo-*N*-dealkyl transformation product despite the fact that they also observed two losses of water.

M10 (*m/z* 278.1733, Δm=−6.47 ppm) was formed through the hydrogenation of MDPV. The fragmentation pattern showed mainly a loss of water at *m/z* 260.1678 (Δm= 12.68 ppm) and a subsequent loss of a propyl radical at *m/z* 217.1126 (Δm=13.36 ppm), in accordance with Paul et al. [30] who elucidated the structure of the same metabolite in human urine. A comparable MS/MS spectrum was reported in an in vitro metabolism study [20], but in our opinion the structure of the metabolite was assigned equivocally to methylcatechol-MDPV, in spite of the fact that the same ions were observed in the MS/MS spectrum. Meyer et al. [21] found two metabolites in human and rat urine with the same exact mass but different fragmentation, so it was attributed to methyl-catechol and demethylenyl-oxo- MDPV.

In the Phase II experiments, glucuronidated conjugates of M2, M3, and M6 were detected, as well as sulphated conjugates of M2. In each case, two isomers were detected resulting from the presence of two hydroxyl groups located on the aromatic ring. The mass errors and the proposed molecular formulas and structures can be found in Table 2. The MS/MS spectra (ESM Fig. S2) showed that the main fragments of the conjugates could be assigned to their non-conjugated equivalent (being M2, M3, and M6). To the best of our knowledge, this is the first study reporting the glucuronidated conjugates of M3 and M6. However, one of the glucuronidated isomers of M2 (demethylenyl-MDPV) as well as a sulphated isomer has been found in in vitro experiments by Strano-Rossi et al. [20]. These authors found also the demethylenyl-methyl-(or methyl catechol-) MDPV-glucuronide and sulphate [20], which were not observed in our study. In human urine, the demethylenyl-methyl-, demethylenyl-methyl-oxo-, demethylenyl-methyl-hydroxy-, demethylenyl-oxo-,

demethylenyl-hydroxy-, besides the demethylenyl- and demethylenyl-methyl-glucuronide-MDPV were found by Meyer et al. [21] and Bertol et al. [33], but were not observed in our study and neither by Strano-Rossi et al. [20]. No sulphated metabolites of MDPV were identified in human urine [21, 33].

Methedrone

The MS/MS spectrum for methedrone (ESM Fig. S3) shows the ions at m/z 176.1072 ($\Delta m = 1.14$ ppm) and 161.0835 ($\Delta m = 0.00$ ppm), as previously reported [3].

M1 (m/z 182.0816, $\Delta m = 2.20$ ppm) was formed through a N- and O-demethylation and a hydroxylation. The loss of NH_3 at m/z 165.0560 ($\Delta m = 8.48$ ppm), the loss of a water molecule at m/z 147.0439 ($\Delta m = -1.36$ ppm) and the loss of CH_2O_2 at m/z 136.0772 ($\Delta m = 11.02$ ppm) demonstrated that the hydroxylation took place in the methyl group bounded in α-position to the nitrogen atom. The hydroxylation in this place was also observed for other cathinones with similar structure [21]. From the ion at m/z 147, loss of CO led to the ion at m/z 107.0509 ($\Delta m = 16.81$ ppm).

Two peaks corresponding to the demethylation of methedrone were observed at m/z 180.1018 ($\Delta m = -3.33$ ppm) and at m/z 180.1023 ($\Delta m = -0.56$ ppm) for M3 and M4, respectively. Characteristic fragment ions were observed at m/z 162.0905 ($\Delta m = -4.94$ ppm) and at m/z 147.0682 ($\Delta m = 2.04$ ppm) for M3, and at m/z 162.0906 ($\Delta m = -4.32$ ppm) and at m/z 147.0673 ($\Delta m = -4.08$ ppm) for M4. Other fragment ions were similar to those observed in the methedrone MS/MS spectrum. Taking into account the log K_{ow} estimated by ChemBio3D Ultra, the first metabolite should correspond to the N-demethylation (M3) and the second one to the O-demethylation (M4). These metabolites were previously found by Mueller and Rentsch [24] after in vitro metabolism experiments of methedrone and in urine from two fatal intoxications [13], but their confirmation was not done by AMS.

M5 (m/z 196.1341, $\Delta m = 2.04$ ppm) corresponded to the reduction of the ketone group of methedrone. A loss of water was observed in the MS/MS spectrum at m/z 178.1230 ($\Delta m = 2.25$ ppm) yielding the most abundant ion. The ion at m/z 146.0958 ($\Delta m = -4.11$ ppm) was observed in the methedrone spectrum as well. The rest of the fragment ions had very low abundance and as such, the m/z could not be measured accurately. This metabolite was not previously reported [24] although the same reaction was noted for other cathinones, such as 4-methylethcathinone [24] and mephedrone [34, 35].

An additional metabolite (M2) at m/z 210.1121 ($\Delta m = -4.28$ ppm) corresponding to a hydroxylation of methedrone was observed in full scan mode. Unfortunately, the compound was not present at high abundance and no MS/MS spectrum could be acquired. Although the position of the hydroxyl group could not be confirmed, it might be located in the methyl group attached to the α-carbon of the nitrogen atom. If so, M2 could be a substrate for the formation of M1 by N- and O-demethylation.

No glucuronidated and sulphated conjugates of methedrone and its Phase I metabolites were detected. However, positive control samples confirmed the reliability of the experimental design.

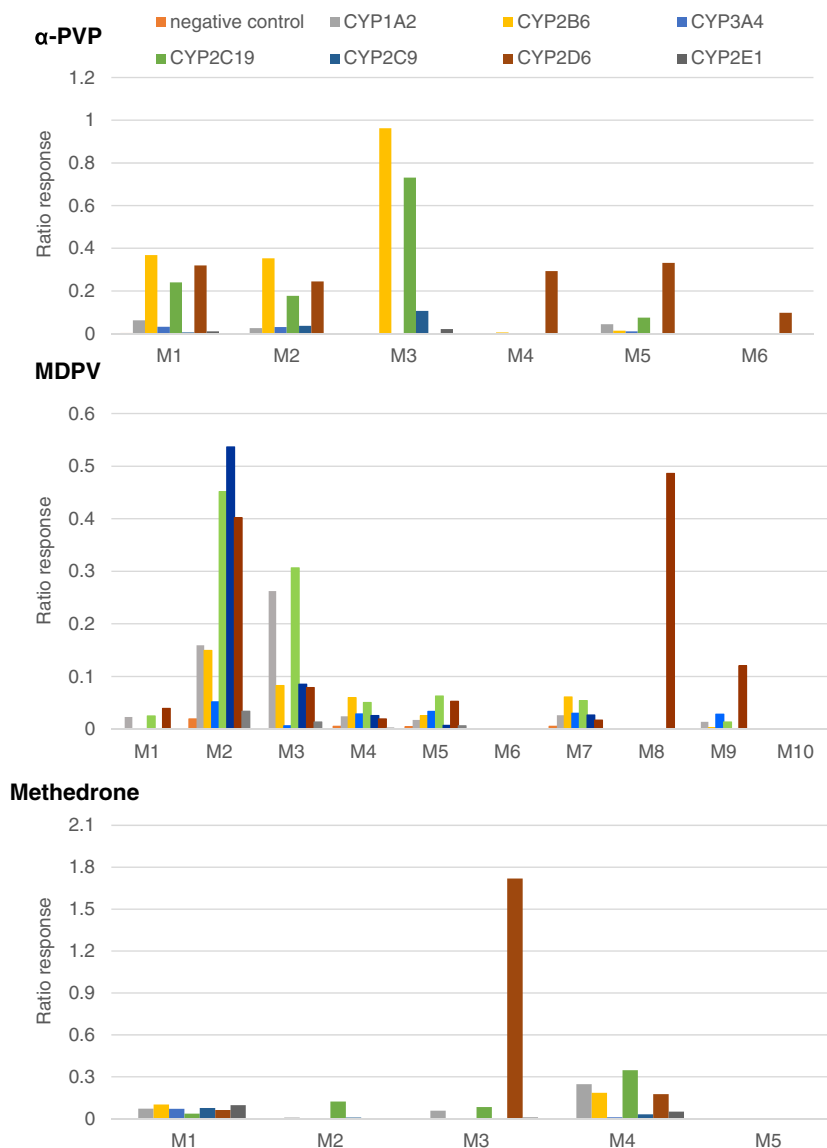## Time, enzyme, and substrate profiles of the metabolites detected

The profiles of the identified metabolites at different incubation times, enzyme concentrations, and substrate concentrations are shown in ESM Figs. S7 to S10. The response of the metabolite is reported as a ratio of the peak area of the metabolite to the area of the IS peak. However, it should be remarked that although useful for discussion purposes, a higher response does not always guarantee a higher concentration of the metabolites as different ESI efficiencies may be expected for different chemical structures. No metabolites were detected in any negative control sample and, in general, an increasing trend in the response was observed with incubation time, enzyme, and substrate concentrations. In some cases, a decrease in the metabolite response was observed, possibly because of their consequent conversion into other metabolites. In the case of MDPV, the response ratios clearly suggest that M2 is the major metabolite of MDPV under the experimental conditions used (ESM Fig. S8). For methedrone, the responses of M2 and M5 were 100 times lower than those of M3, suggesting that M2 and M5 are minor metabolites (ESM Fig. S10).

Human CYP enzymes involved in the metabolism of α-PVP, MDPV, and methedrone

α-PVP

All metabolites identified in the HLM experiments were also formed in human rCYP incubations (Fig. 1). Among the panel of rCYPs tested, rCYP2D6 was the only enzyme responsible for the formation of M4, M5, and M6, and it was a major enzyme in the formation of M1 and M2. rCYP2B6 and rCYP2C19 were the main enzymes responsible for the formation of M1, M2, and M3. Nevertheless, the human hepatic CYP3A4, together with 2B6, 2C19, and 2D6, were reported to catalyze the hydroxylation of the alkyl chain in α-PVP [29]. To the best of our knowledge, the human hepatic CYPs responsible for the formation of all metabolites, except those formed by hydroxylation, were identified here for the first time.

Fig. 1 Ratio response of α-PVP, MDPV, and methedrone metabolites after 1 h-incubations of each drug at 10 μM with a panel of human recombinant CYP enzymes (20 pmol/mL)

MDPV

With the exception of M6 and M10, all metabolites identified in the HLM experiments were found in human rCYPs experiments (Fig. 1). This result suggests that M6 and M10 are likely formed by other enzymes present in the HLM. Among the rCYPs tested, rCYP1A2, rCYP2B6, rCYP2C9, rCYP2C19, and rCYP2D6 were the major enzymes catalyzing the formation of M1, M2, M3, M4, M5, and M7, whereas rCYP2D6 was the main enzyme catalysing the formation of M9 and the only one involved in the formation of M8. Only the rCYPs implicated in the demethylenation of MDPV were previously identified [21]. Recombinant CYP2C19, followed by rCYP2D6 and rCYP1A2, were found to be the main enzymes catalyzing the formation of M2 [21]. Our data show that rCYP1A2, rCYP2C19 and rCYP2D6 played an important role in the formation of M2, but also show that rCYP2B6 and

especially rCYP2C9 were among the most important enzymes involved in the formation of M2. Differences in the experimental design, analytical methods, or both could help explain differences in the human recombinant CYP enzymes found to be responsible for the formation of M2.

Methedrone

With the exception of M4, all metabolites formed incubating methedrone with HLM were also formed by the panel of human rCYP enzymes (Fig. 1). Among the tested panel of human rCYPs, rCYP2D6 was the main enzyme responsible for the N-demethylation of the methedrone producing M3. This data is consistent with what was previously reported for mephedrone in vitro metabolism [34]. Besides rCYP2D6, rCYP1A2, rCYP2B6, and rCYP2C19 were involved in the O-demethylation of methedrone, resulting in M4. The

hydroxylation of methedrone (forming M2) was catalyzed almost exclusively by rCYP2C19. Whereas M1 presented the same response for all rCYPs, M5 was not observed in any sample and or in the negative control. This data is consistent with M5 being a minor metabolite of methedrone produced by HLM, but it could also suggest the involvement of human hepatic CYP enzymes other than those tested.

Proposed metabolic pathways for α-PVP, MDPV, and methedrone

A tentative metabolism pathway of the drugs of interest with CYPs is proposed in Fig. 2.

α-PVP was found to be metabolized by a carbonyl reduction (M6), followed by a hydroxylation in the pyrrolidine ring (M4), a dehydrogenation/oxidation to form a lactam structure (M3), and a subsequent ring opening to form an aliphatic aldehyde combined with an additional hydroxylation in the propyl side chain (M2). α-PVP could be transformed into M5 after two hydroxylations in the pyrrolidine ring, one of them in α-position to the nitrogen atom, followed by an oxidation with a ring opening yielding an aldehyde. Finally, M1 was formed after losing the hydroxyaminobutanal chain of M5 or the pyrrolidine ring of α-PVP. We observed only a glucuronidation of M3 as Phase II reactions. These findings were in agreement with those reported by Tyrkkö et al. [22]. However, formation of M1 and the glucuronidated conjugates of M3 are reported for the first time in the present study, together with the identity of the CYP enzymes involved in the formation of the metabolites. Therefore, our study represents an improvement towards the complete characterization of the pathway of α-PVP metabolism and the prediction of its in vivo metabolism in humans. Urine is a complex matrix in which the identification of metabolites by non-targeted approaches is extremely difficult because of the lack of a control or blank (exactly the same matrix without substance and metabolites) in order to compare with the sample from the user. For this reason, the present work is very relevant in order to add these new metabolites in a database and to look for them in urine samples by targeted approaches.

MDPV was metabolized in a large extension, with an O-demethylenation (M2) as most favorable reaction. However, other pathways were also elucidated (Fig. 2). M2 can be hydroxylated to M1 and subsequently dehydrated to M3. MDPV could also undergo a hydroxylation (M7), two hydroxylations (M9), followed by O-demethylenation and two losses of water (M6). M6 could also be formed from M3 by dehydrogenation in the pyrrolidine ring. Another pathway was the reduction of the carbonyl group of MDPV (M10), followed by hydroxylation in the propyl side chain (M8), hydroxylation of the pyrrolidine ring in α-position to the nitrogen atom, subsequent oxidation yielding ring opening, and formation of an aldehyde group (M4). Finally, M5

could be formed from MDPV or M7 after a loss of the pyrrolidine ring. MDPV underwent Phase II metabolism catalyzed by UGTs and SULTs. In particular, M2, M3, and M6 were glucuronidated yielding two isomeric conjugates, whereas only M2 is sulphated.

Previous in vitro experiments carried out by Strano-Rossi et al. [20] reported that the main metabolites of MDPV were the catechol and the methylcatechol, which were in turn sulphated and glucuronidated. Meyer et al. [21] identified the CYP enzymes responsible for only the conversion of MDPV into its catechol metabolite (M2 in the present study). All other metabolites of MDPV were not described previously in in vitro experiments, though M1, M2, and M10 have been found in human urine [21, 30, 33]. Human rCYP enzymes involved in their formation as well as discrepancies in assigning the structures of the metabolites present in previous studies [21, 33] were clarified. Therefore, the present study not only confirms the previous limited findings about MDPV in vitro metabolism but also substantially improves our understanding of Phase I and Phase II in vitro metabolism of MDPV. Furthermore, it predicts better the in vivo MDPV metabolism and provides a more thorough assignment of the structures of the detected metabolites.

The main pathway observed for methedrone was an N- and O-demethylation resulting in M3 and M4. Hydroxylation of the methyl group attached to the α-carbon of the nitrogen atom (M2) and reduction of the ketone group (M5) were also observed (Fig. 2). The detection of small amounts of M2 can be due to its quick N- and O- demethylation leading to M1. This metabolite can also be formed from M3 after O-demethylation and hydroxylation. These results are in agreement with those described for other similar cathinones [24]. However, only the formation of M3 and M4 has been reported in the sole study investigating the in vitro metabolism of methedrone [24]. Therefore, our study confirms previous findings but it also extends the characterization of the in vitro metabolism pathway methedrone, including the identification of the CYP enzymes involved.

Conclusions

In the present study, the in vitro Phase I and Phase II metabolism of α-PVP, MDPV, and methedrone was investigated using HLM and HLCYT. The major metabolite for MDPV was the catechol, which was further glucuronidated and sulphated. α-PVP and methedrone were preferentially metabolized by monohydroxylation after ketone-reduction and N-demethylation, respectively. The difference in response between the major and the other metabolites of α-PVP and methedrone was not as high as for MDPV metabolites. Nevertheless, all in vitro metabolites should be confirmed with in vivo data because the prevalence of one or other

Fig. 2 Proposed metabolism pathway of α-PVP, MDPV, and methedrone

metabolites may vary with the time after the intake of the drug. Therefore, these results are very useful in order to generate databases as complete as possible for the screening of consumption of NPS through urine analysis.

References

1. Prosser J, Nelson L (2012) The toxicology of bath salts: a review of synthetic cathinones. J Med Toxicol 8:33–42

2. Brandt SD, King LA, Evans-Brown M (2014) The new drug phenomenon. Drug Test Anal 6:587–597

3. Zuba D (2012) Identification of cathinones and other active components of 'legal highs' by mass spectrometric methods. TrAC Trends Anal Chem 32:15–30

4. Coppola M, Mondola R (2012) 3,4-methylenedioxypyrovalerone (MDPV): chemistry, pharmacology, and toxicology of a new designer drug of abuse marketed online. Toxicol Lett 208:12–15

5. Favretto D, Pascali JP, Tagliaro F (2013) New challenges and innovation in forensic toxicology: focus on the "new psychoactive substances". J Chromatogr A 1287:84–95

6. Zaitsu K, Katagi M, Tsuchihashi H, Ishii A (2014) Recently abused synthetic cathinones, α-pyrrolidinophenone derivatives: a review of their pharmacology, acute toxicity, and metabolism. Forensic Toxicol 32:1–8

7. Baumann MH, Partilla JS, Lehner KR, Thorndike EB, Hoffman AF, Holy M, Rothman RB, Goldberg SR, Lupica CR, Sitte HH, Brandt SD, Tella SR, Cozzi NV, Schindler CW (2013) Powerful cocaine-like actions of 3,4-methylenedioxypyrovalerone (MDPV), a principal constituent of psychoactive "bath salts" products. Neuropsychopharmacology 38:552–562

8. Anizan S, Ellefsen K, Concheiro M, Suzuki M, Rice KC, Baumann MH, Huestis MA (2014) 3,4-methylenedioxypyrovalerone (MDPV) and metabolites quantification in human and rat plasma by liquid chromatography-high resolution mass spectrometry. Anal Chim Acta 827:54–63

9. Marusich JA, Antonazzo KR, Wiley JL, Blough BE, Partilla JS, Baumann MH (2014) Pharmacology of novel synthetic stimulants structurally related to the "bath salts" constituent 3,4-methylenedioxypyrovalerone (MDPV). Neuropharmacology 87:206–213

10. Elliott S, Evans J (2014) A 3-year review of new psychoactive substances in casework. Forensic Sci Int 243:55–60

11. Zancajo MR, Brito J, Carrasco MP, Bronze MR, Moreira R, Lopes A (2014) Analytical profiles of "legal highs" containing cathinones available in the area of Lisbon, Portugal. Forensic Sci Int 244:102–110

12. Ibáñez M, Sancho JV, Bijlsma L, Van Nuijs ALN, Covaci A, Hernández F (2014) Comprehensive analytical strategies based on high-resolution time-of-flight mass spectrometry to identify new psychoactive substances. TrAC Trends Anal Chem 57:107–117

13. Wikström M, Thelander G, Nyström I, Kronstrand R (2010) Two fatal intoxications with the new designer drug methedrone (4-methoxymethcathinone). J Anal Toxicol 34:594–598

14. Hasegawa K, Suzuki O, Wurita A, Minakata K, Yamagishi I, Nozawa H, Gonmori K, Watanabe K (2014) Post-mortem distribution of α-pyrrolidinovalerophenone and its metabolite in body fluids and solid tissues in a fatal poisoning case measured by LC-MS/MS with the standard addition method. Forensic Toxicol 32:225–234

15. Nagai H, Saka K, Nakajima M, Maeda H, Kuroda R, Igarashi A, Tsujimura-Ito T, Nara A, Komori M, Yoshida K-I (2014) Sudden death after sustained restraint following self-administration of the designer drug α-pyrrolidinovalerophenone. Int J Cardiol 172:263–265

16. Namera A, Urabe S, Saito T, Torikoshi-Hatano A, Shiraishi H, Arima Y, Nagao M (2013) A fatal case of 3,4-methylenedioxypyrovalerone poisoning: coexistence of α-pyrrolidinobutiophenone and α-pyrrolidinovalerophenone in blood and/or hair. Forensic Toxicol 31:338–343

17. Wyman JF, Lavins ES, Engelhart D, Armstrong EJ, Snell KD, Boggs PD, Taylor SM, Norris RN, Miller FP (2013) Post-mortem tissue distribution of MDPV following lethal intoxication by "bath salts". J Anal Toxicol 37:182–185

18. Murray B, Murphy C, Beuhler M (2012) Death following recreational use of designer drug "bath salts" containing 3,4-methylenedioxypyrovalerone (MDPV). J Med Toxicol 8:69–75

19. de Jager AD, Warner JV, Henman M, Ferguson W, Hall A (2012) LC-MS/MS method for the quantitation of metabolites of eight commonly-used synthetic cannabinoids in human urine—an Australian perspective. J Chromatogr B 897:22–31

20. Strano-Rossi S, Cadwallader AB, de la Torre X, Botrè F (2010) Toxicological determination and in vitro metabolism of the designer drug methylenedioxypyrovalerone (MDPV) by gas chromatography/mass spectrometry and liquid chromatography/quadrupole time-of-flight mass spectrometry. Rapid Commun Mass Spectrom 24:2706–2714

21. Meyer MR, Du P, Schuster F, Maurer HH (2010) Studies on the metabolism of the α-pyrrolidinophenone designer drug methylenedioxy-pyrovalerone (MDPV) in rat and human urine and human liver microsomes using GC-MS and LC-high-resolution MS and its detectability in urine by GC-MS. J Mass Spectrom 45:1426–1442

22. Tyrkkö E, Pelander A, Ketola R, Ojanperä I (2013) In silico and in vitro metabolism studies support identification of designer drugs in human urine by liquid chromatography/quadrupole-time-of-flight mass spectrometry. Anal Bioanal Chem 405:6697–6709

23. Shima N, Katagi M, Kamata H, Matsuta S, Sasaki K, Kamata T, Nishioka H, Miki A, Tatsuno M, Zaitsu K, Ishii A, Sato T, Tsuchihashi H, Suzuki K (2014) Metabolism of the newly encountered designer drug α- pyrrolidinovalerophenone in humans: identification and quantitation of urinary metabolites. Forensic Toxicol 32:59–67

24. Mueller DM, Rentsch KM (2012) Generation of metabolites by an automated online metabolism method using human liver microsomes with subsequent identification by LC-MS (n), and metabolism of 11 cathinones. Anal Bioanal Chem 402:2141–2151

25. Tukey RH, Strassburg CP (2000) Human UDP-glucuronosyltransferases: metabolism, expression, and disease. Ann Rev Pharmacol 40:581–616

26. Gamage N, Barnett A, Hempel N, Duggleby RG, Windmill KF, Martin JL, McManus ME (2006) Human sulfotransferases and their role in chemical metabolism. Toxicol Sci 90:5–22

27. Tautenhahn R, Patti GJ, Rinehart D, Siuzdak G (2012) XCMS Online: a web-based platform to process untargeted metabolomic data. Anal Chem 84:5035–5039

28. Mardal M, Meyer MR (2014) Studies on the microbial biotransformation of the novel psychoactive substance methylenedioxypyrovalerone (MDPV) in wastewater by means of liquid chromatography-high resolution mass spectrometry/mass spectrometry. Sci Total Environ 493:588–595

29. Sauer C, Peters FT, Haas C, Meyer MR, Fritschi G, Maurer HH (2009) New designer drug α-pyrrolidinovalerophenone (PVP):

studies on its metabolism and toxicological detection in rat urine using gas chromatographic/mass spectrometric techniques. J Mass Spectrom 44:952–964

30. Paul M, Ippisch J, Herrmann C, Guber S, Schultis W (2014) Analysis of new designer drugs and common drugs of abuse in urine by a combined targeted and untargeted LC-HR-QTOFMS approach. Anal Bioanal Chem 406:4425–4441

31. Uralets V, Rana S, Morgan S, Ross W (2014) Testing for designer stimulants: metabolic profiles of 16 synthetic cathinones excreted free in human urine. J Anal Toxicol 38:233–241

32. Regan SL, Maggs JL, Hammond TG, Lambert C, Williams DP, Park BK (2010) Acyl glucuronides: the good, the bad, and the ugly. Biopharm Drug Dispos 31:367–395

33. Bertol E, Mari F, Boscolo Berto R, Mannaioni G, Vaiano F, Favretto D (2014) A mixed MDPV and benzodiazepine intoxication in a chronic drug abuser: determination of MDPV metabolites by LC-HRMS and discussion of the case. Forensic Sci Int 243:149–155

34. Pedersen A, Reitzel L, Johansen S, Linnet K (2013) In vitro metabolism studies on mephedrone and analysis of forensic cases. Drug Test Anal 5:430–438

35. Meyer MR, Wilhelm J, Peters FT, Maurer HH (2010) Beta-keto amphetamines: studies on the metabolism of the designer drug mephedrone and toxicological detection of mephedrone, butylone, and methylone in urine using gas chromatography-mass spectrometry. Anal Bioanal Chem 397:1225–1233